The Impact of Various Heating Rates on Real-Time Degree of Hybrid Fire Simulation

Faranak Faghihi [iD]* *and Markus Knobloch* [iD], *Chair of Steel, Lightweight and Composite Structures, Ruhr-Universität Bochum, Universitätsstraße 150, 44801 Bochum, Germany*

Abstract. Global fire performance of structures in fire is proven to be more advantageous in many cases of engineering practice than the prescriptive fire resistance based on isolated structural member testing. Hybrid fire simulation (HFS) is a novel well-suited method trending in recent years for analysis of global performance of structures in fire. In the principles of this method, the part of a structure which has unknown behavior or is uncertain to be numerically modeled (subjected to fire) would be physically tested, while the rest of the structure is numerically simulated. HFS method enables capturing the beneficial interaction mechanisms evolving between fire-exposed structural members and the adjacent cooler substructure. Due to the continuous temperature increase in a fire test and the existing thermal inertia as well as the rate- and temperature-dependent material behavior of structures exposed to fire, a real-time performance in hybrid fire simulation counts as a necessity. This challenge is more critical for hybrid fire simulations with higher applied heating rates relevant to structural fire engineering. Within scope of this paper, (a) a robust and rigorous approach for real-time HFS is presented; (b) a series of proof-of-concept studies of different hybrid fire simulations with various applied heating rates are carried out for a thermomechanical benchmark problem; (c) the important results of four representative hybrid fire simulations with relevant heating rates to structural fire engineering are discussed; (d) the importance of an appropriate calculation method for stiffness update of the fire-exposed structural member over HFS procedure is highlighted, and e) the precision and accuracy of the applied HFS approach with respect to interface error and real-time degree are evidenced.

1. Introduction

The prescriptive methods based on isolated, single structural component fire testing can often not realistically estimate the global fire behavior of structures when exposed to fire. It is due to the fact that in single-member fire testing and pre-

---

* Correspondence should be addressed to: Faranak Faghihi, E-mail: Faranak.Faghihi@rub.de

scriptive component-based approaches, the effects of evolving fire on boundary conditions and loading are neglected, and the interaction mechanisms between the fire-exposed structural member and the adjacent cooler substructure are missing. Therefore, performance-based design approach, counts as a more appropriate method for analysis of global fire performance of structures. Costly full-scale fire tests on entire structures and the purely numerical simulations on global structures still afflicted with uncertainties regarding precise modeling of material and boundary conditions in fire, spark the necessity of an alternative suitable method. Hybrid fire simulation (HFS) is a novel well-suited alternative method for performance-based design approach of global structures. In this method, the structural member exposed to fire is physically tested while the rest of the structure would be numerically modeled. The numerical simulation and physical fire test would be coupled in a way that the numerical simulation controls and updates the data achieved from the physical fire test. Due to the fact that ongoing fire test is not halted and elevated-temperature material properties are usually time, heating-rate and strain-rate dependent, the hybrid fire simulation needs to be performed in a real-time procedure.

Despite the application of hybrid simulation since decades in the earthquake engineering, hybrid fire simulation still deals with some complications and has been thoroughly investigated just since recent years. Some early attempts were made for hybrid fire simulation as pioneering ideas back in 1980s and 1990s [1, 2], which although paved the way for study of global performance of structures subjected to fire, were not successful and did not continue. Korzen et al. [3] suggested the substructuring method and highlighted the beneficial interaction effects of the surrounding structure for fire-exposed members. Various other researchers also studied HFS in recent years; but only few of them were capable to apply physical fire tests [4–8], while others presented a virtual conceptual framework for their proposed methodology of HFS [9, 10]. No one in previous researches considered and bolded an appropriate calculation method for stiffness update of the fire-exposed structural member. Several shortcomings could be listed by scrutinizing the state-of-the-art studies: The non-negligible errors at the interface of the numerical and physical substructures due to lack of iterative method in the solution procedure [4, 9], studying only elastic material properties and skipping material nonlinearities [5], neglecting the effect of plasticization and material nonlinearities on response of HFS and degrading stiffness of the fire-exposed member, as well as lack of a pure physical setup for validation of the proposed HFS methodology [7]. Only Schulthess et al. [8] considered recently a rigorous framework for HFS which was also purely physically validated [11]; however, the stiffness of the fire-exposed element was considered to be constant, equal to initial stiffness of the element at ambient temperature during the HFS procedure, contradicting the reality in fire incidents. Owing to this assumption, the real-time degree of HFS was not fulfilled when traversing through nonlinear material behavior [8]. Faghihi et al. [12, 13] assessed the rigorous thermal coupling in methodology of HFS as an advancement to [8]. Recently, Faghihi [14] stressed the necessity of an appropriate method of stiffness update in HFS solution procedure for the degrading physical element in fire with respect to real-time thermal-induced phenomena arising during HFS.

In this paper, a robust and rigorous methodology of real-time HFS is firstly presented. Second, an appropriate benchmark structure consisted of high-strength steel S690QL is introduced, and the setup and framework of HFS established for this research are explained. Four representative HFSs with various applied heating rates relevant to structural fire engineering are thoroughly discussed, and the computational challenges for real-time fulfillment of HFSs with high heating rates as well as the accomplished solutions for these challenges are clarified. At the end, the accuracy of the proposed HFS approach is investigated. This study proves the robustness and competence of the proposed method of real-time HFS for further enhancements in structural fire engineering.

2. Brief Overview of Hybrid Fire Simulation Methodology

The state-of-the-art studies performed regarding HFS are to be conceptually categorized in two different approaches: (a) the first approach determines the hybrid fire simulation as centered around the physical fire test and the numerical simulation of the rest of structure is considered as a part of the control system's function of the ongoing fire test [4, 7, 9]. This approach would be limited to defined problems and laboratory-specific hybrid fire simulations which cannot generically implement the methodology of HFS on structures in fire; (b) the second approach considers HFS as an extended numerical model of the structure which in an ongoing analysis run controls, updates, and integrates the data from the uninterruptible fire test [5, 6, 8]. This approach is developed based on principles of hybrid simulation in earthquake engineering and is not confined to problem- and laboratory-specific analyses.

Within scope of this paper, the second approach is followed, since it eliminates the instabilities arising in first approach due to the computationally detached substructures, and considers a generic approach for global analysis of the structures in fire bearing a great potential as a rigorous tool. In this paper, an incremental solution procedure with an iterative method is applied to the hybrid model as an extended numerical model in order to investigate the equilibrium equation of forces and the displacement compatibility at the interface of numerical and experimental substructures. The thermomechanical response of the structure is analyzed by dividing each increment of the HFS procedure into a thermal stage followed by a mechanical one [14, 15]. In each increment of the ongoing analysis run, an iterative solution method is applied to fulfill the mechanical equilibrium of the structure by data achieved from continuous fire test, with additional consideration of temperature synchronization at the interface of substructures. In the thermal stage of each increment and by start of heating in the furnace of fire test, a target temperature would be sent to physical test from numerical model, while the testing machine is in force-hold control mode. By heating and reaching to target temperature, a thermal expansion occurs in the physical specimen representing fire-exposed element in structure, although no thermal deformation is happened in user-defined element equal to physical specimen in model. That causes a mismatch

in displacement compatibility between physical and numerical substructures which requires iterations in consecutive mechanical stage to repair the incompatibility. The iterative method in the incremental solution procedure provides the force and displacement compatibility and enables a proper update of the fire-exposed substructure's degrading stiffness. In the proposed HFS methodology in this paper, the stiffness of fire-exposed element would be updated with respect to temperature- and rate-dependent phenomena happening during the fire test. This counts as the main enhancement of the proposed method in current paper in comparison to the state-of-the-art studies. The incremental solution procedure with iterative method and appropriate update method of fire-exposed elements' stiffness in HFS methodology can provide temperature and time synchronicity as well as the equilibrium of forces and displacements at the interface of numerical and physical substructures which result in diminished interface errors.

3. Framework of Hybrid Fire Simulation

In this section, a thermomechanical benchmark structure necessary for validation of HFS approach is presented. In addition, the framework and setup of HFS consisting of numerical and physical parts are explained.

3.1. Thermomechanical Benchmark Structure

The generic thermomechanical benchmark problem for validation of HFS has to be a sufficiently sophisticated yet expediently simple structure which can represent the structures partially exposed to fire. This benchmark structure is worth to be validated by purely physical testing, in order to enable the verification of HFS methodology and the beneficial interaction mechanisms arising in the global structure. In this research, the benchmark structure to study is adopted from [8]; it is due to the fact that this benchmark structure complies with the proof-of-concept prerequisites and is validated already by full-physical testing by Neuenschwander et al. [11].

The benchmark structure comprises a laboratory-scale simply supported beam connected at its mid-span through a hinge to a truss element. The truss element is the element exposed to fire, while the beam element counts as the adjacent cooler substructure. The benchmark structure is exposed to an external load P_0 applied in the mid-span of the beam element. This external load is internally distributed, with respect to the stiffness proportionalities of truss and beam, to the truss element and beam supports based on their load shares, so that the static equilibrium is always fulfilled in the system, $F_{truss} + 2F_{beam} = P_0$. The deflection formed in the mid-span of the beam, w, is equal in this case to the axial displacement of the truss element u_{tr}.

Figure 1 displays the thermomechanical benchmark structure as well as the determined loading protocol. Alike conventional fire tests and fire incidents, the loading protocol includes a mechanical loading followed by a thermal one (Fig. 1left). First, an external load $P(t)$, starting from 0 to P_0 in time $t_0 - t_1$, is linearly applied at ambient temperature θ_0. Thereafter, by start of the heating
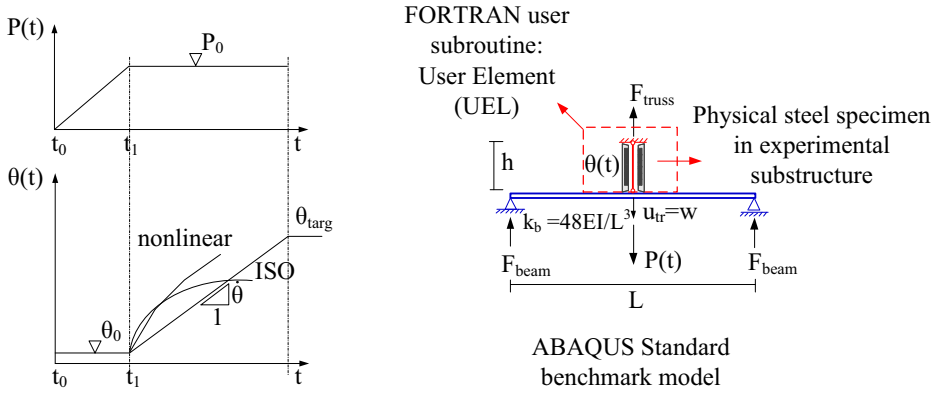
Figure 1. **Schematic overview of the thermomechanical benchmark structure (right), mechanical and thermal loading protocol in current hybrid fire simulation (left).**

phase, P_0 is taken constant and the heating is started from t_1. The thermal loading $\theta(t)$ is defined as a target predetermined temperature–time curve with the heating rate of $\dot{\theta}$, subjected to truss element. By start of the heating and development of temperature- and rate-dependent material and physical properties in the truss element, such as thermal expansion, stiffness and strength degradation as well as high temperature creep, the load in truss element starts to degrade and would be redistributed to beam supports. After complete degradation of truss element by fire exposure and its complete failure, the whole external load P_0 would be carried by beam supports.
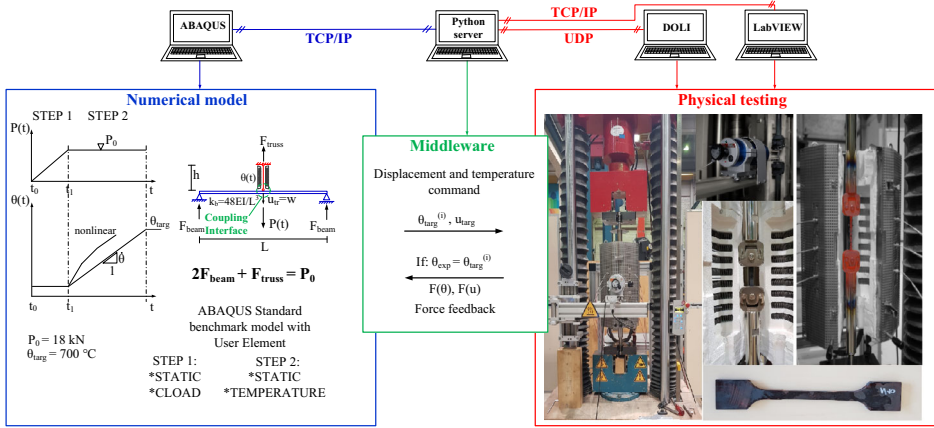
3.2. Hybrid Fire Simulation Setup

In this section, different subparts of HFS setup are elaborated on: the numerical simulation is performed in FE-software ABAQUS/Standard with the fire-exposed structural member as a user-defined element written with Fortran in user subroutine UEL. Beam is modeled with the Euler–Bernoulli beam element B23 with the length of 600 mm and flexural rigidity of $EI = 163.17 \times 10^6$ kNmm². The physical element in the fire test is a dog-bone shaped specimen with total length of 170 mm, central gauge length L_0 of 45 mm and initial nominal cross section area of $A_0 = 54$ mm² constituted of steel S690QL. Material properties of applied steel is adopted from same batch of S690QL steel plates with thickness of 12 mm [16, 17], derived by means of steady-state tests at different temperatures 20, 400, 550, 700, and 900 ℃. The specimen is put in a universal testing machine (UTM) (manufacturer Schenck). The UTM includes an integrated load cell calibrated as class 1 in accordance with [18], with a maximum capacity of 250 kN. The electromechanical UTM is running with controlling DOLI software. The specimen is fixed in the machine with high-temperature resisting specimen holders and additional tension rods connecting the specimen setup to loading frame and the moving cross-head of the machine. The specimen is surrounded by an electric three-zone furnace

(manufacturer Könn) controlled with LabVIEW software. A high-temperature resisting extensometer (manufacturer MAYTEC), calibrated in accordance with [19], is fixed with its two ceramic rods on the specimen measuring the central deformation at the gauge length of specimen. Therefore, the displacement of the physical element (fire-exposed member) refers in this research to the measured deformation by extensometer u_{exp}, which equals to truss displacement u_{tr} and mid-span deflection of the beam w at the interface of numerical and physical substructures. The interaction and automated communication between numerical simulation and physical element's controlling software (DOLI for universal testing machine and LabVIEW for furnace, respectively) are enabled through a middleware software acting as a server written in python. This server has the task to transfer data between numerical and physical substructures, i.e. it sends target temperature and displacement from numerical simulation (ABAQUS model) to furnace and UTM machine, respectively and receives the corresponding force from machine back to numerical model. The communication between numerical simulation and server, as well as the communication between furnace's controlling software and server, are established by a TCP/IP communication, while the communication between the controlling software of the universal testing machine and server is a UDP connection. TCP/IP communication and UDP connection provide an error-free real-time transfer of data between numerical model and physical setup, which aids further the real-time performance of hybrid fire simulation. Further details regarding the algorithm of these communication protocols are explained in [14]. Figure 2 presents the overview of the HFS setup implemented and applied in this research.

4. Hybrid Fire Simulations with Different Applied Heating Rates in Thermal Loading

Applied heating rates relevant to structural fire engineering in hybrid fire procedure count as a remarkable parameter in investigating the real-time degree of HFS. Due to existing thermal inertia in the uninterruptible physical fire test in HFS, it is important to fulfill the real-time necessity and synchronization of the analysis with respect to applied heating rate of thermal loading. This aspect gains more importance for HFS with faster elevation of temperatures. In this section, four accomplished hybrid fire simulations with various applied heating rates as proof-of-concept representatives are presented. The regarding information are shown in Table 1. In all HFSs, the initial load-shares between fire-exposed truss element and adjacent cooler beam with respect to their stiffness proportionalities are 90 and 10%, respectively. Also, the initial load ratio $\mu = F_{t,amb}/F_{y,0.2\%}$ in truss element, according to truss element's force with respect to actual yielding load of truss at ambient temperature is 40% in all the simulations.

In the performed analyses, the procedure and physical fire test are controlled with fire-exposed specimen's temperature following the determined target temperature curve. Although it is unlike real fire incidents and usual fire tests which are monitored and controlled with air temperature, it provides the benefit to investi-
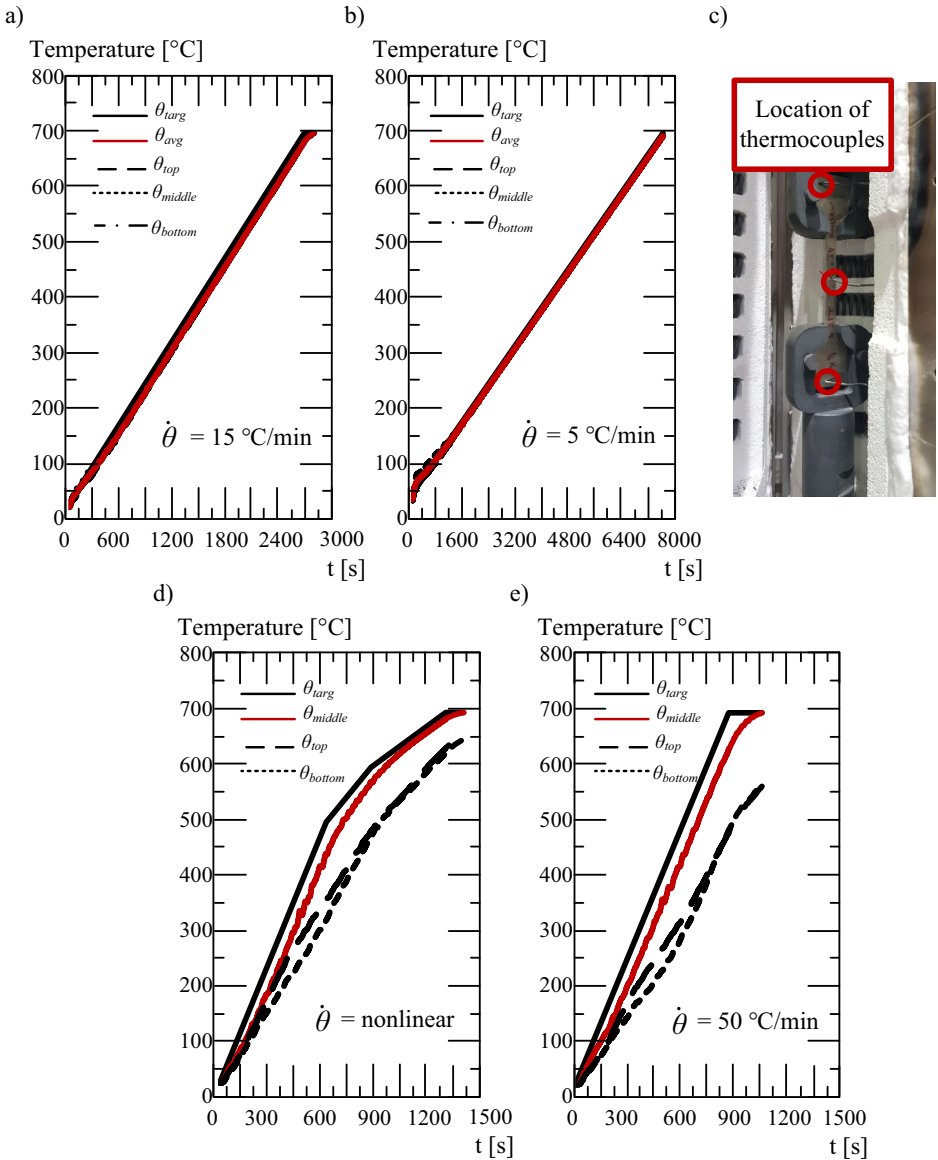
Figure 2. **Thermomechanical setup implemented and applied for HFS.**

Table 1
Overview of the Four Presented Hybrid Fire Simulations

No [–]	P_0 [kN]	$F_{t,amb}$ [kN]	μ [%]	θ_{targ} [C]	Heating rate [C/min]	Solver method
HFS 1	18	16.3	40	700	15	Initial stiffness
HFS 2	18	16.3	40	700	5	Updated stiffness
HFS 3	18	16.3	40	700	nonlinear	Updated stiffness
HFS 4	18	16.3	40	700	50	Updated stiffness

gate the induced temperature-dependent phenomena more thoroughly with respect to the well-known temperature in the specimen at each instance of the HFS incremental solution procedure. According to Table 1, final target temperature is 700°C. HFS 1 and HFS 2 are defined by linear target temperature curves with heating rates of 15 and 5°C/min, respectively. In these cases, due to a unified temperature distribution over the specimen by the applied heating rates, the specimen temperature $\theta_{specimen}$ is recognized as the mean value of measured temperatures by thermocouples at top, middle and bottom zone of the specimen, $\theta_{avg} = (\theta_{top} + \theta_{middle} + \theta_{bottom})/3$ (Fig. 3a and b).

HFS 3 owns a nonlinear step-wise temperature curve with the purpose of emulating ISO standard fire curve [20] with respect to inherent limitations of the furnace in fire test: first, a linear increase from ambient temperature up to 500°C is determined with the heating rate of 50°C/min; second, a linear temperature curve with the reduced heating rate of 25°C/min is applied from 500 up to 600°C; at the end, temperature curve proceeds with the linear heating rate of 15°C/min up to the target temperature of 700°C.

a)

Temperature [°C]

$\dot{\theta}$ = 15 °C/min

b)

Temperature [°C]

$\dot{\theta}$ = 5 °C/min

c)

Location of thermocouples

d)

Temperature [°C]

$\dot{\theta}$ = nonlinear

e)

Temperature [°C]

$\dot{\theta}$ = 50 °C/min

Figure 3. (a) Target temperature curve as well as the specimen's temperature for HFS 1, (b) target temperature curve as well as the specimen's temperature for HFS 2, (c) location of the thermocouples on the surface of the specimen, (d) target temperature curve as well as the specimen's temperature for HFS 3, (e) target temperature curve as well as the specimen's temperature for HFS 4.

HFS 4 goes on with a linear target temperature curve by heating rate of 50˚C/min, which is the highest applicable heating rate to specimen with respect to inherent limitations of furnace. In two latter HFSs, the specimen's temperature distribution is not unified and a thermal gradient exists over the length of specimen, as shown in Fig. 3d and e. It is owing to the fact that thermocouples measuring the specimen's temperature have a tip contact to the specimen's surface and the two ones at the top and bottom zones of specimen are located in a position enclosed by specimen clamps (Fig. 3c). For consistency of results, the position of thermocouples at top, middle and bottom zones of the specimen are identical in all four HFSs. Therefore, in high heating rates, the specimen cannot heat up equally in different zones in a specific time period and solely the surface would be heated. With respect to Fig. 3d and e, it is shown that middle zone's temperature follows most closely the target temperature curve. Hence, for HFS 3 and 4, the middle zone temperature is assigned to the specimen temperature controlling the hybrid fire procedure: $\theta_{specimen} = \theta_{middle}$. Figure 3 present the target temperature curves as well as the measured temperatures on specimen's surface in different zones for all HFSs.

5. Results and Discussion

In this section, the results regarding thermomechanical response of hybrid fire simulations as well as their precision are presented and discussed.

5.1. Thermal-Induced Phenomena Affecting Response of HFS

In hybrid fire simulations, the thermomechanical response of the structure and the consequent load redistribution in the global structure are to be investigated. During the ongoing fire test in the hybrid fire procedure, various thermal-induced phenomena arise either individually or simultaneously in the fire-exposed element. So, the response of HFS can be assigned to different contributing stages with respect to various temperature- and time-dependent phenomena. These stages are identified and demonstrated in Fig. 4. Figure 4a shows the stress in fire-exposed element vs. specimen's middle-zone temperature for four HFSs. Additionally, the 0.2% yielding strength, $f_{y,0.2\%,\theta}$, and the proportional limit, $f_{p,\theta}$, at different temperatures taken from [17, 18] are displayed. Figure 4b shows the tangent stiffness of the fire-exposed specimen, which is calculated as the moving average of the measured points with a centered data sample consisting of 21 data points, over specimen's middle-zone temperature for HFS 3 and 4 as most critical analyses with highest heating rates.

Among contributing stages, the first stage refers to dominant effect of restrained thermal expansion reducing the stress in fire-exposed element. This stage is marked up to 400˚C for all HFSs. It is also verified by the constant tangent stiffness of the specimen at this range for HFS 3 and 4 shown in Fig. 4b. (measured by moving average of a centered data sample consisting of 21 data points). The fluctuations observed in tangent stiffnesses in this stage are related to the inevitable oscillations in force measurement in the machine at initial temperatures
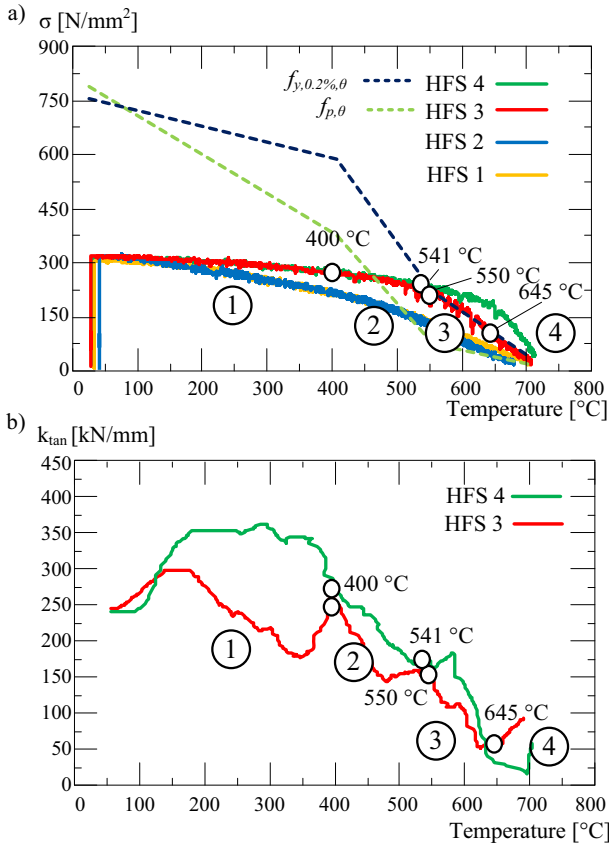
Figure 4. (a) Stress-specimen's middle-zone temperature for four respective hybrid fire simulations, (b) tangent stiffness of the specimen over specimen's middle-zone temperature for HFS 3 and HFS 4.

and the method of measurement, calculation and modification of the tangent stiffness in our approach.

In second stage, the dominant effect of stiffness degradation additionally arises which is due to temperature-dependent reduction of Young's modulus. In HFS 1 and 2, the stresses in specimen are below the yielding strength; therefore, no plasticity occurs in these analyses and the thermomechanical response of these hybrid fire simulations is specified with the two mentioned stages. For HFS 3 and 4, second stage is marked up to 550℃ and 541℃, respectively. Gradual decrease of the stiffness in this stage (Fig. 4b) also testifies prevailing effect of temperature-dependent stiffness degradation.

As it is shown in Fig. 4, the stress values differ even before onset of plasticity at initial stages for HFS 1 and 2 (with lower heating rates) and HFS 3 and 4 (higher

heating rates). This difference even in elastic loading can be explained due to the non-unified temperature distribution along the specimen in HFS 3 and 4 in comparison to the uniformly heated specimens in HFSs with slower heating (HFS 1 and 2). So, in HFSs with faster heating, the proper thermal and rate-dependent deformations are not formed due to surface heating resulting in smaller displacements in truss element and mid-span deflection of beam and consecutive higher stresses in truss element (physical specimen).

Third stage starts once the stresses in fire-exposed specimen surpass the yielding strength and is determined by additional dominant effect of strength degradation. This is also confirmed by a steep decrease of tangent stiffness in HFS 3 and HFS 4. This stage continues in HFS 3 up to 645℃ from which the stresses again reach below the temperature-dependent 0.2% yielding strength $f_{y,0.2\%,\theta}$. For HFS 4, this stage proceeds till the end of hybrid fire simulation. Only at the end at 697℃, decreased tangent stiffness (reached almost to zero) starts to gradually stabilize. This period refers to increments in hybrid fire procedure which do not have a proper thermal stage with no to small thermal expansion that will be explained further.

For HFS 3, the fourth stage is defined from 645℃ up to the end in which the stresses are below the yielding strength in elastic region and the stiffness stabilizes gradually.

In addition to aforementioned thermal-induced physical properties, high temperature creep can play an important role in thermomechanical response of HFS. Nevertheless, due to temperature- and stress-dependency of creep, it cannot be specifically assigned to last stages and the simultaneous prevailing effect of creep besides other temperature-dependent properties may affect the response of hybrid fire simulation as well as the resulting load redistribution in the global structure. In Fig. 5, the first thermal derivative of thermal deformation $du_{exp,th}/d\theta$ vs. specimen's middle-zone temperature are shown for four HFSs. This thermal deformation refers to developed thermal expansion in thermal stage of each increment in the HFS incremental solution procedure. According to Fig. 5, this thermal derivative increases initially by start of thermal expansion and then is approx. constant for HFS 1 which governs in elastic range. On the other hand, this default constant value starts to deviate for HFS 2 and HFS 3 in 420℃ and 460℃, respectively. These points arise before the onset of any plastic deformations, which can evidence the effect of high temperature creep deformations. High temperature creep is surely expectable in HFS with slow heating rate of 5℃/min (HFS 2). In HFS 3, the deviating point 460℃, is the transition point of the heating rate in specimen (from 50℃/min to 25℃/min). Switch of heating rate justifies the evolution of high temperature creep deformations as well as more proper thermal elongations. This aspect complies with response of HFS 4 in which no creep is expected with respect to the high heating rate 50℃/min.

5.2. Computational Challenges of Real-Time HFS

Real-time synchronization is a crucial necessity for performance of hybrid fire simulation. It is owing to the fact that in hybrid fire simulation, an ongoing fire

du/dθ [mm/°C]
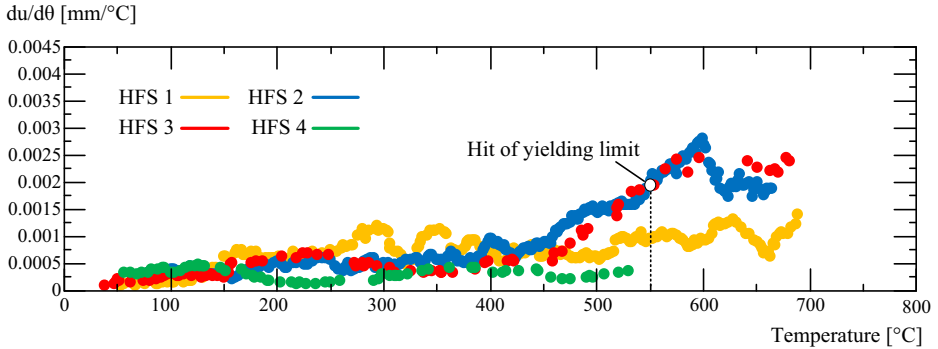
Figure 5. Thermal derivative of the thermal elongation with respect to specimen's middle-zone temperature for HFS 1, 2, 3, and 4.

test proceeds and the furnace would not be halted, like in case of real fire incidents and usual fire tests. Therefore, because of the existing thermal inertia, the temperature in mechanical stage of one increment may exceed the incremental target temperature of next increment. In this case, the thermal stage of the next increment would be contracted causing no or small thermal expansion in that increment. That causes a mismatch in displacement compatibility in subsequent mechanical stage of the regarding increment, which requires an iteration to rectify the mismatch. Therefore, in incremental solution procedure of HFS, iterations needed in mechanical stage have to be solved properly, robustly and sufficiently fast to maintain the synchronization and real-time fulfillment of hybrid fire simulation.

In case of plastic loading and initiation of plasticization, more number of iterations may be needed to fulfill the equilibrium equation of forces and displacement compatibility in the increments. More required iterations and the uninterruptible temperature evolution in the fire test lag temperature consistency and mismatch the compatibility of solution even more. Therefore, the real-time degree and well-synchronicity of HFS procedure deems more challenging for hybrid fire simulations with higher heating rates, e.g. HFS 4 with heating rate of 50°C/min.

Figure 6 shows the force vs. displacement graph of fire-exposed element for all HFSs. This displacement is the measured one in specimen u_{exp}. In addition, the converged values at the end of each increment of numerical procedure are shown with marked points. As shown in Fig. 6a and b, the increments in HFS 1 and 2 are with few number of iterations and the converged values at end of each increment of solution procedure (black marked points) are close to each other. This shows the ease of convergence in the iterative solution procedure of HFS for the ones with lower heating rates remaining in elastic behavior. For HFS 3 with higher nonlinear heating rates, as shown in Fig. 6c, the converged data points get more distant in few plastic increments in comparison to other increments. That evidences the existence of more iterations for increments with high plasticity. In Fig. 6d, for HFS 4, it is observed that one increment is more critical to be converged since the convergence points are more distant in comparison to the rest of
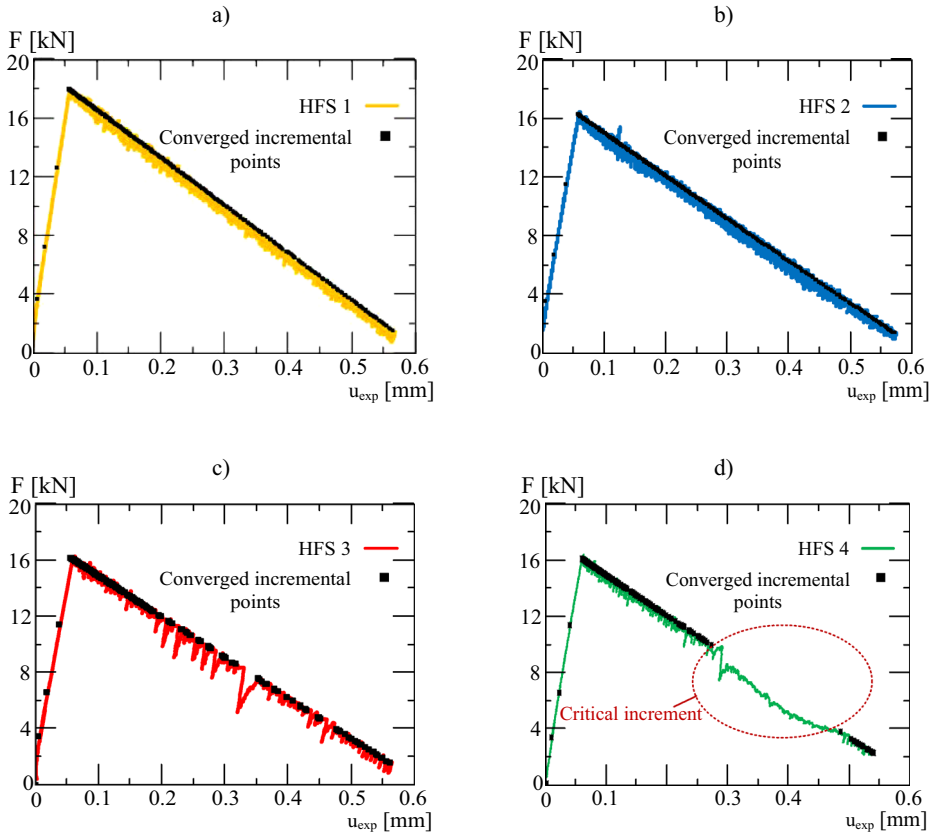
Figure 6. **Force–displacement graph derived for fire-exposed element of all HFSs in addition to converged data points in numerical simulation at end of each increment.**

increments. This increment consists of 11 iterations (as shown in [21]), takes 153 s long and results in 74℃ temperature lag. So, the necessity for a computational solver to increase the convergence of iterative solution procedure in HFSs with higher heating rates and to fulfill their real-time degree is crucial. In the following, this computational procedure is explained and is further presented for challenging increment of HFS 4.

5.2.1. Numerical Predictor Solver In increments with contracted thermal stage, the mismatch corrections in mechanical stage, which cause iterations, are usually smaller than controlling limit precision (1 μm: micrometer) of the measuring device (extensometer) in physical fire test. Therefore, sending a new target displacement to the machine leads only to oscillations in machine and cannot restore the correct resulting force. As a solution in the iteration of mechanical stage, we use a numerical predictor solver which solves the resulting force in that iteration

purely numerical with respect to the tangent stiffness of the previous iteration. This helps the increment to be successfully converged. The increments which have applied predictor mechanism due to suppressed thermal stage, are generally faster than the increments owning normal thermal stage. That can help the rate of hybrid fire simulation in order to resynchronize again in time and temperature. So, the increments after increments with contracted thermal stage, possess again a normal thermal stage with thermal expansion and are compatible with ongoing fire test in furnace. In Fig. 6d, the consecutive increments after the critical delaying increment of HFS 4 have contracted thermal stage, and therefore, use the numerical predictor solver which helps to compensate the lagged time and temperature and to finalize the simulation successfully converged.

5.2.2. Appropriate Method of Stiffness Update for Fire-Exposed Specimen Computational parameters are main factors to be enhanced in order to improve the real-time degree of the hybrid fire simulation. Numerical predictor solver, as mentioned in previous section, additionally aids to improve the desynchronizations over the procedure. The most essential computational parameter is the method of update of stiffness for fire-exposed element. This gains much more importance for hybrid fire simulations with high applied heating rates. According to [14, 15], the update of fire-exposed element's stiffness is necessary, especially for cases of plasticization and nonlinear behavior. The update of stiffness in each iteration of the incremental solution procedure can be as follows:

$$k^{(j)} = \frac{F^{(j)} - F^{(j-1)}}{u^{(j)} - u^{(j-1)}} \tag{1}$$

with j as iteration counter. In addition, we propose a modification to omit the effect of inevitable oscillations on force measurement in the testing machine. Therefore, a threshold of $\pm 10\%$ (determined experimentally) is to be considered to encase the deviations in stiffness update of fire-exposed element; i.e. for case which $k^{(j)}$ is differentiated more than $\pm 10\%$ of tangent stiffness in previous iteration, $k_{tan}^{(j-1)}$, the updated tangent stiffness of the iteration is $k_{tan}^{(j)} = (1 \pm 0.1) \times k_{tan}^{(j-1)}$.

For hybrid fire simulations with higher heating rates, an additional computational modification is suggested and explained in this paper. This computational modification applies for increments with high plasticity. Owing to the effect of strength degradation in cases of plasticity and the steep decrease of stiffness in this case (Fig. 4b), the tangent stiffness greatly reduces reaching to almost zero and drives in some increments to negative values. The random negative values of stiffness may yield the procedure to divergence and consequent abortion of the simulation. The proposed modification is considered to omit these upcoming negative values: for all iterations in plasticity which possess a negative stiffness as $\partial F/\partial u$, the updated tangent stiffness would be considered as zero. This solution has come up due to the fact that the slope of constitutive stress–strain curve gets almost constantly zero by hitting the yielding point in plasticization. This considered modification is applied in the iterative numerical solution procedure of HFS 4. So,

for all plastic increments with negative stiffness $\partial F/\partial u$, the updated tangent stiffness is modified to zero. This improvement has helped the critical delaying increment of HFS 4 (Fig. 6d) to converge successfully. Figure 7 shows the calculated stiffness of the fire-exposed specimen (solid line) and the updated tangent stiffness with considered modification (dot line) for all iterations of the critical increment shown in Fig. 6d.

5.3. Precision of Proposed Approach of HFS

In this section, the precision of the proposed approach of HFS in this paper is demonstrated and discussed. The accuracy can be investigated with two different parameters: the interface error in displacement and force responses at the interface of numerical and physical substructures, and the real-time degree and well-synchronicity of the HFS procedure.

5.3.1. Interface Error The proposed approach of HFS is taken error-free if the compatibility of displacements and forces at the interface of numerical and physical substructures at the end of each converged increment is completely achieved. On the other hand, since last iteration of almost each increment is solved purely numerical with the predictor solver, an inevitable error exists at the interface of numerical and physical substructures with respect to the precision limit of the measurement devices in the physical setup. These absolute errors can be characterized as the mismatch of displacement and forces at the interface of substructures, respectively: $\delta u_{abs} = u - u_{exp}$ and $\delta F_{abs} = F - F_{exp}$. Another parameter to investigate the accuracy of HFS method at the interface of substructures is specified as relative force error which is the ratio of absolute force error to physical element's force $\delta F_{rel} = \delta F_{abs}/F_{exp}$.

Figure 8 shows the absolute displacement error, δu_{abs} (a), absolute force error, δF_{abs} (b), and the relative force error δF_{rel} (c) vs. fire-exposed specimen's displacement u_{exp} (displacement measured by extensometer) at the end of each increment for HFS 4. These errors are shown for HFS 4 as the representative hybrid fire simulation since it is the most critical analysis with highest heating rate studied in this paper.

The implementation of numerical predictor solver in the last iteration of almost each increment arises from the fact that the displacement correction in the last iterations is smaller than the controlling precision limit (1 μm) of the measurement device (extensometer) in the physical test. Hence, a threshold of 1 μm is also determined to check the absolute displacement error at the end of each increment.

As it is shown from Fig. 8a, the absolute displacement error lies soundly under the threshold of 1 μm. The exception is in increments with only one iteration which have contracted thermal stage and are solved completely with numerical predictor solver. In this case, the mismatch and error exceeds up to 1.6 μm. In addition, it is displayed that for last iterations of increments which are dealt with physical test, the absolute displacement error is less than 0.1 μm, equal to resolution of measurement device (extensometer) evidencing very sound accuracy.
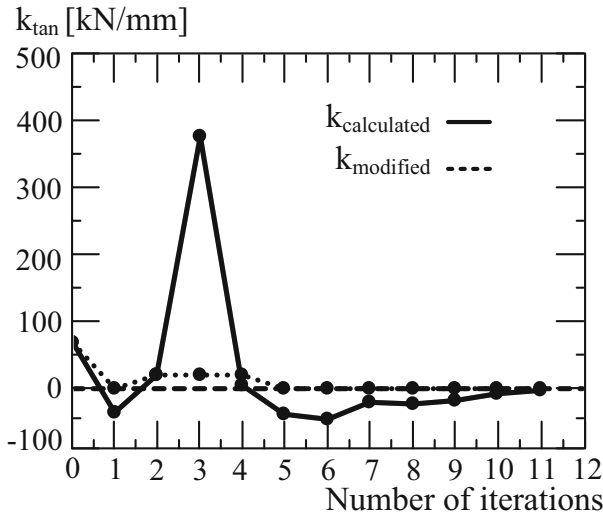
Figure 7. Calculated and modified tangent stiffness of the specimen in the iterative numerical procedure of critical increment of HFS 4.

The absolute force error in Fig. 8b is also with a sound accuracy below the determined threshold, which is defined with respect to the threshold of absolute displacement error (1 μm) multiplied with tangent stiffness of physical substructure in each iteration. Relative force error complies with a sound threshold of 2% as well; except at the very end in which F_{exp} is greatly decreased resulting in high rise of relative error. The threshold is surpassed also in some initial increments; it can be justified due to contracted thermal stages and improper thermal expansion as well as the oscillations of force in measurements of the machine.

5.3.2. Real-Time Degree Real-time degree and temperature synchronization are another parameter with which the robustness and precision of the proposed approach of HFS can be investigated. Figure 9a shows the temperature difference between specimen's middle-zone temperature and the determined nominal target temperature in numerical simulation for the four presented HFSs. Also, the ratio of the physical time which a HFS procedure takes to the assumed time of numerical simulation is demonstrated in Fig. 9b for all HFSs. This ratio is shown in closer scale for HFS 3 and 4 with highest heating rates in Fig. 9c. Additionally, the physical time duration as well as its mean value are presented in Fig. 9d to g for all HFSs.

Figure 9a testifies the temperature compatibility between specimen temperature and nominal target temperature over increments of HFSs. In HFS 4, only in the critical delayed increment (Fig. 6d) these temperatures deviate up to 74°C, but it is compensated again due to abovementioned computational solvers and modifications. In Fig. 9b, as it is shown, the physical time and numerical simulation time fit perfectly together for HFS 1 and 2. Also with a closer look to HFSs with high
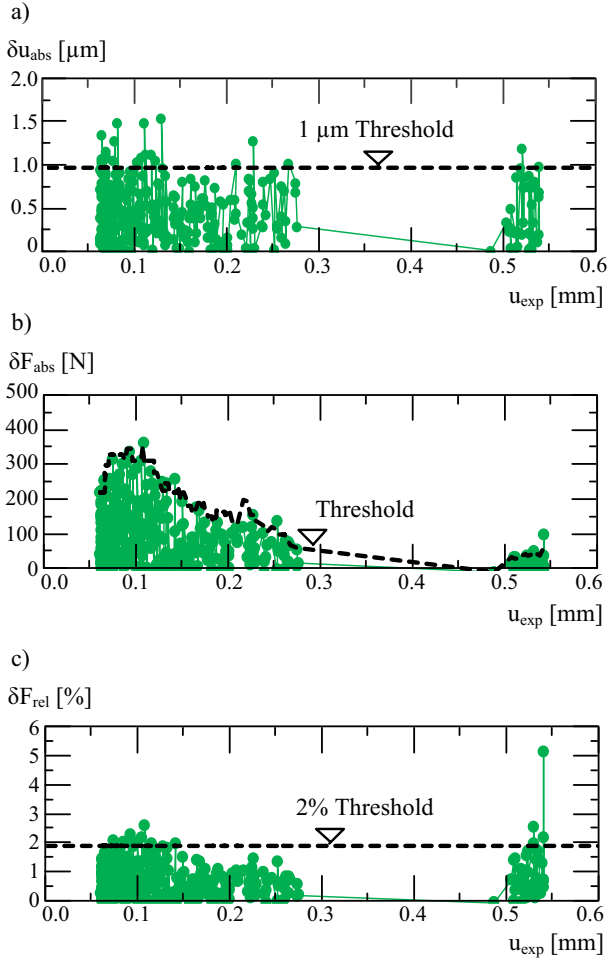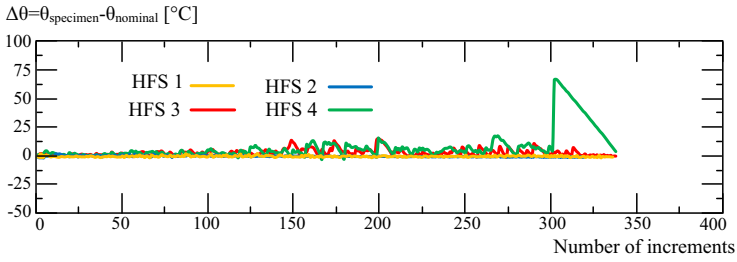
Figure 8. (a) Absolute displacement error of HFS 4, (b) absolute force error of HFS 4, (c) relative force error of HFS 4.
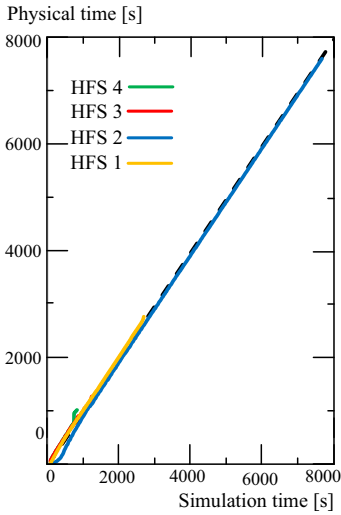
heating rates in Fig. 9c, it can be seen that physical time and numerical simulation time for HFS 3 with nonlinear heating rate have a unit linear ratio with a good accuracy. In HFS 4, the numerical simulation time gets lagged in the mentioned critical increment (Fig. 6d) from the ongoing physical test. This explains the deviation of the physical time from the simulation time during this increment. Thereafter, due to the compensating solver method for increments with contracted thermal stages and faster convergence, the physical and simulation times converge again to each other, getting closer in next increments till the end.

From Fig. 9d to g, it is shown that the mean value of physical time complies with the determined/performed heating rates of HFS 1 to 4. That evidences the sound accuracy of real-time degree for the proposed HFS approach in this paper.

a)

Δθ=θ$_{specimen}$-θ$_{nominal}$ [°C]

HFS 1
HFS 2
HFS 3
HFS 4

Number of increments

b)

Physical time [s]

HFS 4
HFS 3
HFS 2
HFS 1

Simulation time [s]

c)

Physical time [s]

HFS 4
HFS 3

Simulation time [s]

d)

Δt$_{real}$ [s]

Δt$_{mean}$ = 8.3 s

Number of increments

e)

Δt$_{real}$ [s]

Δt$_{mean}$ = 23.4 s

Number of increments

f)

Δt$_{real}$ [s]

Δt$_{mean}$ = 8.3 s
Δt$_{mean}$ = 4.5 s
Δt$_{mean}$ = 2.7 s

Number of increments

g)

Δt$_{real}$ [s]

Δt$_{mean}$ = 3.1 s

Number of increments
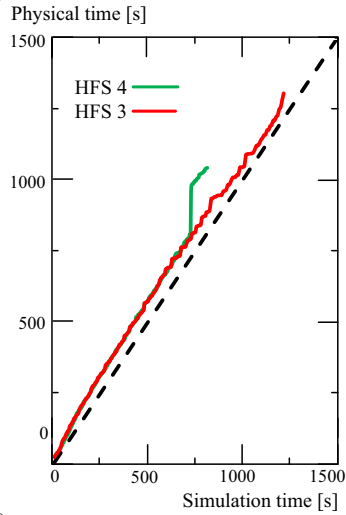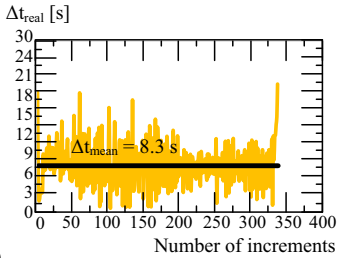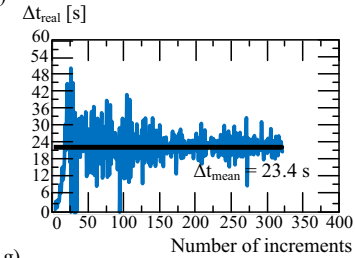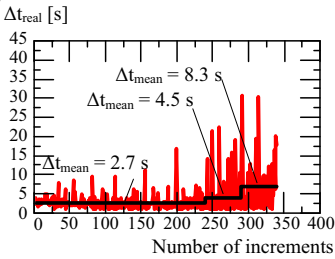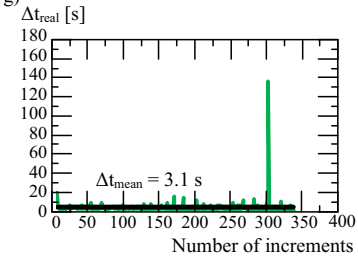
◄**Fig. 9.** **(a) Difference of specimen's temperature and nominal target temperature of simulation for four HFSs, (b) physical time of the hybrid fire simulation over nominal simulation time for four HFSs, (c) physical time of the hybrid fire simulation over nominal simulation time for HFS 3 and 4, (d) physical time in each increment and its mean value for HFS 1, (e) physical time in each increment and its mean value for HFS 2, (f) physical time in each increment and its mean value for HFS 3, (g) physical time in each increment and its mean value for HFS 4.**

6. Conclusions

Hybrid fire simulation (HFS) is an appealing well-suited alternative for analysis of global fire performance of structures. Among state-of-the-art studies, only few researches have succeeded to implement and apply physical fire tests in the proposed framework for HFS. However, a rigorous real-time HFS analysis considering all thermal-induced phenomena arising in linear and nonlinear material behavior and in temperature ranges relevant to structural fire engineering is still missing in the state-of-the-art findings and researches. This paper has presented a robust and rigorous methodology and framework for real-time HFS which is capable of dealing with computational and experimental challenges happening during HFS. In this paper, for the first time, a HFS with applied heating rate of $50°C/min$ and its upcoming challenges have been investigated. Four representative HFSs with various heating rates relevant to structural fire engineering have been analyzed and their results have been discussed. The computational challenges and the necessity of real-time performance of HFSs with higher heating rates have been highlighted. In addition, the necessity of an appropriate method for stiffness update of the fire-exposed substructure has been explained and the additional modifications for update of physical substructure's stiffness in cases of HFSs with higher heating rates have been scrutinized.

This paper proves that the HFS method applying the update of fire-exposed element's tangent stiffness as well as considering the required modifications for calculation of stiffness is a strong tool and can significantly lead to well-synchronized results. The proposed HFS method is proven to be an accurate and robust approach with respect to the errors at the interface of numerical and physical substructures as well as the time and temperature synchronization and real-time degree of the procedure. This research serves as a valuable step, paving the path for further developments in conducting large-scale HFS on structures. It has to be noted that in hybrid fire simulations with large-scale structural members the loading structure and its size also influence the physical tests. Hence, measured deformations in the physical tests include also the deformations of the loading structure affected by stiffness of loading structure as well. Nevertheless, the update of stiffness method with necessary modifications with respect to requirements and limitations of fire test, is undoubtedly essential for a realistic interpretation of structural fire behavior of physical structural members in HFS. The proposed method for update of tangent stiffness in iterative solution procedure of HFS can also be

applied in case of using other structural materials such as concrete; however, the required thresholds and modifications for update of temperature-dependent degrading stiffness are to be respectively adjusted.

Acknowledgements

Funding

Data Availability Statement

The raw/processed data required to reproduce these findings cannot be shared at this time as the data also forms part of an ongoing study. The relevant data can be made available on request.

Declarations

Competing interest The authors declare that they have no known competing financial interests or personal relationships that could have appeared to influence the work reported in this paper.

Open Access

References

1. Kiel M (1989) Entwicklung einer intelligenten Prüfmaschine für brandbeanspruchte Gesamttragwerke. In: Braunschweiger Brandschutz-Tage

2. Hosser D, Ameler J, Dorn T, Gensel B (1993) Entwicklung einer "lntelligenten Prüfmaschine" zur Untersuchung von Gesamttragwerken unter lokaler Brandbeanspruchung. Abschlussbericht zur 2. Phase des Forschungsvorhabens

3. Korzen M, Magonette G, Buchet P (1999) Mechanical loading of columns in fire tests by means of the substructuring method. In: Proceedings of the eighth interflam conference, pp 911–914

4. Mostafaei H (2013) Hybrid fire testing for assessing performance of structures in fire—application. Fire Saf J 56:30–38. 10.1016/j.firesaf.2012.12.003

5. Whyte CA, Mackie KR, Stojadinovic B (2016) Hybrid simulation of thermomechanical structural response. J Struct Eng 142. https://doi.org/10.1061/(ASCE)ST.1943-541X.0001346

6. Wang X, Kim RE, Kwon O-S, Yeo I (2018) Hybrid simulation method for a structure subjected to fire and its application to a steel frame. J Struct Eng 144:04018118-1–04018118-11. 10.1061/(ASCE)ST.1943-541X.0002113

7. Mergny E, Franssen J-M (2020) Real-time multi degrees of freedom hybrid fire testing using Pi control. In: Conference proceedings of the 11th international conference on structures in fire. The University of Queensland, Australia, pp 77–88

8. Schulthess P, Neuenschwander M, Mosalam KM, Knobloch M (2020) A computationally rigorous approach to hybrid fire testing. Comput Struct 238:106301–106320. 10.1016/j.compstruc.2020.106301

9. Sauca A, Gernay T, Robert F, Tondini N, Franssen J-M (2018) Hybrid fire testing: discussion on stability and implementation of a new method in a virtual environment. J Struct Fire Eng 9:319–341. 10.1108/JSFE-01-2017-0017

10. Qureshi R, Elhami-Khorasani N, Gernay T (2019) Adaption of active boundary conditions in structural fire testing. J Struct Fire Eng 10:504–528. 10.1108/JSFE-12-2018-0042

11. Neuenschwander M, Schulthess P, Mosalam KM, Knobloch M (2022) Validating hybrid fire testing with full-physical twin experiments. Proceedings of the Royal Society A 478. https://doi.org/10.1098/rspa.2022.0180

12. Faghihi F, Neuenschwander M, Knobloch M (2019) A computational framework for thermal coupling in hybrid fire simulation. In: COUPLED VIII: proceedings of the VIII international conference on computational methods for coupled problems in science and engineering, pp 757–767

13. Faghihi F, Knobloch M (2019) Thermal coupling in hybrid fire simulation. In: Advances in engineering materials, structures and systems: innovations, mechanics and applications, pp 1897–1902. https://doi.org/10.1201/9780429426506-327.

14. Faghihi F (2022) Advanced implementation of hybrid fire simulation. Doctoral thesis. https://doi.org/10.13154/294-9761

15. Faghihi F, Knobloch M (2022) Global structural fire analysis of steel structures implementing hybrid fire simulation. In: 8th symposium structural fire engineering. TU Braunschweig, Germany, pp 199–218

16. Neuenschwander M, Scandella C, Knobloch M, Fontana M (2017) Modeling elevated-temperature mechanical behavior of high and ultra-high strength steels in structural fire design. Mater Des 136:81–102. 10.1016/j.matdes.2017.09.041

17. Knobloch M, Uszball S (2021) CoolFire-Mechanische Materialeigenschaften für die Abklingphase von Naturbrandszenarien. Research Report, DASt-IGF N20915

18. Metallic materials—calibration and verification of static uniaxial testing machines—part 1: tension/compression testing machines—calibration and verification of the force-measuring system (ISO 7500-1:2018) (2018). German version EN ISO 7500-1:2018
19. Metallic materials—tensile test—part 4: verification of extensometers used in uniaxial testing. (1994). German version EN 10002-4:1994
20. ISO 834-1:1999 (1999) ISO (International Organization for Standardization). Fire resistance test—elements of building construction—part 1: general requirements
21. Faghihi F, Knobloch M (2022) Rigorous implementation of real-time hybrid fire simulation applying high heating rates of thermal loading. In: 12th international conference on structures in fire (SiF 2022), pp 553–563